

Review

Recent advancements in the molecular design of deep-red to near-infrared light-absorbing photocatalysts

Minling Zhong¹ and Yujie Sun^{1,*}

SUMMARY

Photocatalysis has traditionally relied on photocatalysts that primarily absorb short-wavelength ultraviolet-visible (UV-vis) light. However, recent advancements have led to the development of photocatalysts that can absorb deep-red to near-infrared light. These near-infrared photocatalysts (NIR-PCs) offer distinct advantages over traditional UV-vis photocatalysts, including deeper tissue penetration and reduced interference from competing absorption processes. Herein, we summarize the latest advancements in their molecular design based on three activation mechanisms: one-photon absorption, triplet-triplet annihilation upconversion, and two-photon absorption. This review aims to present not only various organic transformations facilitated by NIR-PCs but also the diverse molecular engineering strategies that have been employed in the design and development of NIR-PCs, particularly focusing on those with exceptional absorption capabilities in the NIR region. Finally, a brief overview of the current challenges and opportunities for future explorations of NIR photocatalysis is presented, underscoring the growing significance of NIR-PCs in advancing the frontiers of photocatalysis.

INTRODUCTION

The power of photon has been well recognized and harnessed across various fields, including synthesis,^{1–8} catalysis,^{9–13} solar cell,^{14–16} luminescence sensing,^{17–19} and bioimaging.^{20,21} Even though light-driven organic transformations have been known for centuries, photocatalytic reactions were not widely investigated until the last few decades. Thanks to extensive studies in organic and inorganic molecular photocatalysts and the elegant design of photocatalytic systems,⁸ in recent years, photocatalysis has appeared as a powerful platform to realize various synthetic reactions, such as reductive dehalogenation,^{22,23} radical cyclization,²⁴ oxidative biaryl coupling,²⁵ and α -functionalization of arenes and amines,³ allowing previously inaccessible reaction pathways to be explored and exhibiting a tremendous impact on organic synthesis.^{2,4} For instance, photoredox catalysis has facilitated the discovery of otherwise challenging synthetic strategies for drug synthesis and biomolecule modification.⁷ In particular, the spatiotemporal nature of light irradiation as the sole driving force has enabled photocatalytic reactions specifically appealing for site-selective bioconjugation and protein labeling in biological settings, especially when the employed photocatalysts can absorb the light of wavelengths longer than those absorbed by nucleotides, sugars, and amino acids found in biology. Such an advantage allows for the selective delivery of photons to photocatalysts, enabling precise spatiotemporal control over reactivity in complex biological systems.

THE BIGGER PICTURE

Challenges and opportunities

- The design of NIR light-absorbing photocatalysts via one-photon absorption should prioritize synthetic simplicity while maintaining a high extinction coefficient in the NIR region and competent excited-state redox power.
- For those following the triplet-triplet annihilation upconversion mechanism, there is a need to develop more energy-matched sensitizer/annihilator pairs and find strategies to protect the triplet species from oxygen quenching. Another possibility is to optimize the energy transfer process to create simpler and more efficient upconversion systems.
- It is of critical importance to design competent NIR light-absorbing photocatalysts with large two-photon absorption cross-sections and high photocatalytic efficiency, enabling their excitation by inexpensive and readily available NIR LEDs.

Traditional photocatalysts have primarily focused on harnessing ultraviolet-visible (UV-vis) light, corresponding to about 51% of the solar spectrum.^{26,27} However, the remaining half, the near-infrared (NIR) region (700–2,500 nm), represents an underexploited spectrum due to its low photon energy and the limited NIR light absorption of conventional photocatalysts.^{28,29} Indeed, many molecular photocatalysts, such as expensive metal-containing $[\text{Ru}(\text{bpy})_3]^{2+}$ (bpy = 2,2'-bipyridyl), $[\text{Ir}(\text{dF}(\text{CF}_3)\text{ppy})_2(\text{dtbpy})]^+$ ($\text{dF}(\text{CF}_3)$ ppy = 2-(2,4-difluorophenyl)-5-(trifluoromethyl)pyridine, dtbpy = 4,4'-di-tert-butyl-2,2'-bipyridine), and organic dyes like 4CzIPN (1,2,3,5-tetrakis(carbazol-9-yl)-4,6-di-cyanobenzene), have been developed for a variety of photocatalytic reactions. A close analysis of their photophysical properties suggests that Ir-based photocatalysts typically exhibit strong absorption in the UV region with a weak absorption tail in the visible region (blue light), while Ru-based complexes possess relatively red-shifted absorption but still most likely no substantial absorption beyond 500 nm. Even though several organic photocatalysts (e.g., rose bengal and eosin Y) can absorb photons in the wavelength range of 500–600 nm, their limited lifetimes, redox potentials, and stability issues pose concerns regarding long-term applications. Regardless of the innate photophysical properties of each widely used photocatalyst, a common feature is that most of them do not operate effectively under NIR light irradiation.

From an energy perspective, one-photon absorption (OPA) in the UV-vis region is usually required to populate the desirable excited states of most photocatalysts with an energy of 50–80 kcal/mol, which are able to drive many organic transformations.⁵ However, the utilization of UV-vis light has intrinsic limitations such as low penetration through media (for instance, only the reaction medium proximal to the vessel wall within 2 mm will experience irradiation in visible light-driven reactions)³⁰ and competing absorption by reaction substrates and co-catalysts.³¹ In particular, UV-vis light suffers from limited penetration into human tissue, rendering a great challenge for *in vivo* applications. In contrast, NIR light shows the best penetration through human tissue.^{32–34} As most biomolecules (e.g., DNA, amino acid, protein, and sugar) do not absorb NIR photons and hence are inert to NIR light activation, minimal perturbation or damage to biomolecules would be anticipated under NIR light irradiation. Therefore, the development of NIR light-activatable photocatalysts represents an attractive strategy for light-driven biomolecule modification.

In response to the underutilization of NIR light, recent decades have witnessed a surge in research aimed at enhancing NIR light-driven photocatalysis. Researchers have explored various strategies to capture and convert this spectrum of light more effectively, including the development of narrow-band-gap semiconductors, upconversion (UC) systems, and NIR light-responsive chromophores. Despite a wealth of literature reviewing the principles and progress in NIR photocatalysis,^{26–28,35} there remains a critical need for continuous innovation, particularly in the realm of molecular design. This precision-driven approach involves fine-tuning the chemical structures of photocatalysts or components within the photocatalytic systems to maximize their NIR light absorption and hence optimize the photocatalytic activity. In this review, we emphasize the molecular design strategies and methods that enable precise control over NIR light-driven photocatalysis. These strategies are delineated based on three distinct activation modes, including OPA,³⁶ triplet-triplet annihilation UC (TTA-UC),³⁷ and two-photon absorption (TPA). By focusing on photocatalytic systems with excitation wavelengths ranging from 620 to 850 nm, this review aims to summarize the recent advancements, address ongoing challenges, and highlight novel opportunities in the field of deep-red to NIR photocatalysis, offering a forward-looking view into the potential of this emergent and vital area of photocatalysis.

¹Department of Chemistry, University of Cincinnati, Cincinnati, OH 45221, USA

*Correspondence: yujie.sun@uc.edu

<https://doi.org/10.1016/j.chechat.2024.100973>

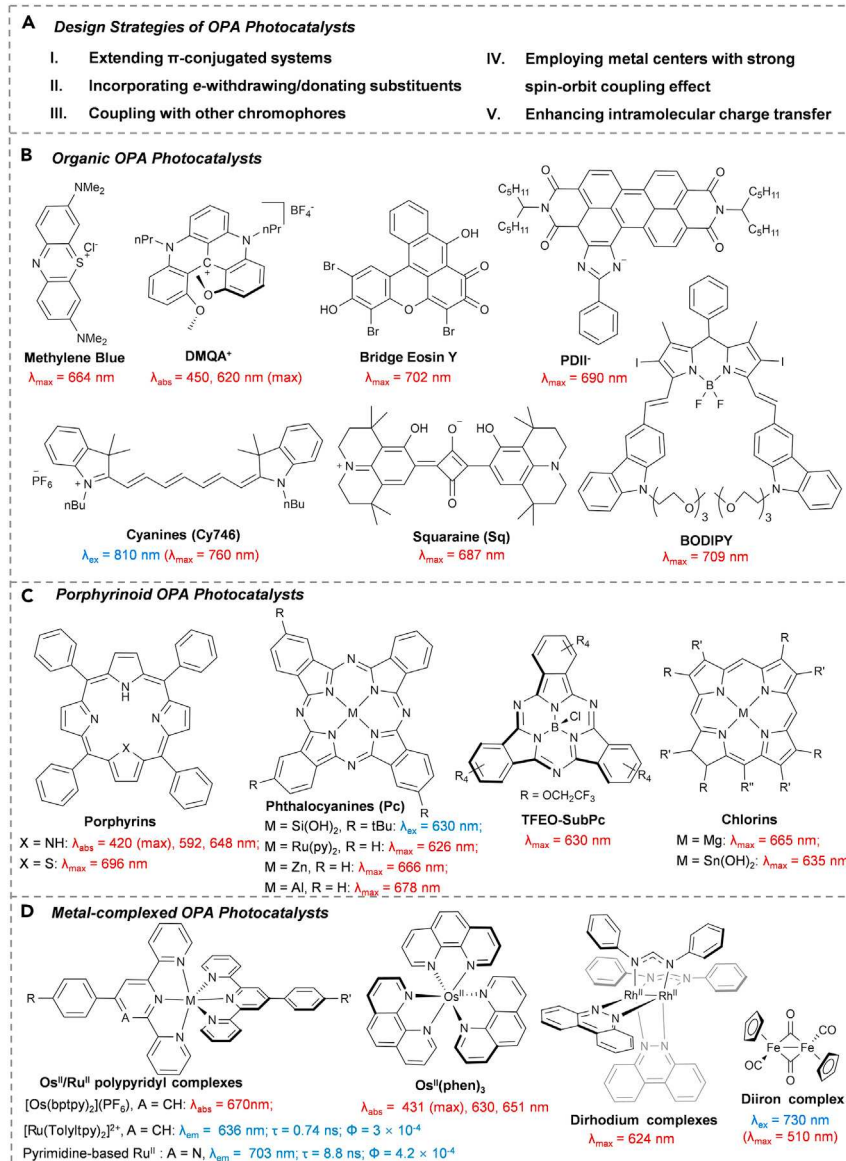


Figure 1. Molecular structure of OPA photocatalysts

- (A) Design strategies of OPA photocatalysts.
- (B) Organic OPA photocatalysts.
- (C) Porphyrinoid OPA photocatalysts.
- (D) Metal-complexed OPA photocatalysts.

OPA

Given the important roles played by conventional organic and organometallic chromophores in visible photocatalysis, many researchers have endeavored to extend their absorption toward longer wavelengths through various chemical modifications and use them as deep-red to NIR photocatalysts (NIR-PCs). The overall design strategies include extending π -conjugated systems, incorporating electron-withdrawing/donating substituents, directly coupling with other chromophores,³⁸ employing metal centers with pronounced spin-orbit coupling effects, and enhancing intramolecular charge transfers (Figure 1A).

Organic dyes

Organic dyes have garnered attention as effective photocatalysts in NIR photocatalysis since the early 2000s (Figure 1B). These dyes typically possess extended π -electron delocalization, a structural feature that is instrumental in absorbing long-wavelength photons of the NIR spectrum. The absorption of these photons facilitates the initiation of electron- or energy-transfer processes to drive a variety of chemical transformations.

Methylene blue (MB), a commonly used organic dye, is known for its ability to absorb red light with an absorption maximum at 664 nm, making it a suitable agent for NIR photocatalysis.³⁹ In a seminal study in 2000, Ferroud and colleagues pioneered the use of MB as a deep-red photocatalyst, demonstrating its capability to facilitate the photooxidation of piperidine and pyrrolidine derivatives^{40,41} as well as the indolizine ring.⁴² Further expanding its application scope, MB has also been shown to act as an electron acceptor in catalyzing the $Z \rightarrow E$ isomerization of azobenzenes.⁴³ Building upon these precedent examples, more recent studies have explored modifications to enhance MB's performance and stability. Notably, in 2021, the Amara group investigated the immobilization of MB on silica nanoparticles as a strategy to protect the catalysts from deactivation.⁴⁴ This innovative approach resulted in a heterogeneous catalyst that exhibited improved performance in the photooxidation of citronellol, outperforming its homogeneous counterpart. More recently, the Zhao group discovered that an MB analog (NMB⁺) exhibited strong photoredox reactivity.⁴⁵ It was found capable of selectively cleaving thermodynamically stable N=N bonds under low-energy excitation using a 655 nm laser. The proposed mechanism involves a novel consecutive two-photon stepwise absorption process. Initially, NMB⁺ absorbs a red photon to generate a triplet excited state ($^3\text{NMB}^{+*}$). This is followed by continuous two-electron reduction steps leading to the formation of a reduced species (LNMB), which then complexes with the azo substrate, enabling the absorption of a second red photon and the subsequent cleavage of the azo bond. Notably, this photocatalytic process can be performed in aqueous solutions or hypoxic cells, paving the way for new bioorthogonal strategies for azo bond cleavage and drug delivery applications.

N,N'-Dialkyl-1,13-dimethoxyquinacridinium (DMAQ⁺) represents a class of stable carbocation ions renowned for their role as NIR emitters.⁴⁶ A key feature of DMAQ⁺ is its helical structure, which significantly contributes to its high stability as a photocatalyst.⁴⁷ In addition, DMAQ⁺ dyes possess adjustable electrochemical, photophysical, and chiroptical properties. These properties can be finely tuned through the introduction of peripheral auxochrome substituents, offering a versatile toolkit for customization according to specific photoredox catalytic needs.^{48,49} In 2020, the Gianetti group showcased that DMAQ⁺ could engage in both oxidative and reductive quenching processes under red LED irradiation ($\lambda_{\text{ex}} = 640$ nm).⁵⁰⁻⁵² In a follow-up study, the Gianetti group further expanded the applications of DMAQ⁺ by employing it in the [3+2] cyclization of cyclopropylamines with alkenes and alkynes, illustrating the broad potential of DMAQ⁺ in facilitating novel photoredox catalysis reactions.⁵³

The modification of chromophore structures represents an innovative approach to extend the optical absorption properties of established dyes into the NIR region. By ingeniously adjusting the molecular architecture, researchers have successfully shifted the absorption spectra of several well-known dyes, enabling their application in NIR-induced photocatalytic reactions. A prime example of this strategy involves eosin Y, traditionally characterized by its absorption peak at 539 nm and widely

used in green-light-induced photocatalysis.⁵⁴ In 2022, the Tanioka group developed a variant of eosin Y featuring an extended π -conjugation system.⁵⁵ This modification induced a bathochromic shift, extending the dye's absorption maximum to 702 nm and rendering it capable of catalyzing arylation reactions with aryl diazonium salts under mild NIR irradiation. Furthermore, iodinated BODIPY dyes were popular visible-light-absorbing photoredox catalysts⁵⁶ and prominent in photodynamic therapy (PDT).⁵⁷ In 2016, the Han group synthesized a carbazole-substituted BODIPY molecule with a broad NIR absorption band (600–800 nm) and applied it to NIR-responsive PDT.⁵⁸ Afterward, the Duan group explored its application in NIR photooxidation of benzylamine derivatives, sulfides, and aryl boronic acids.⁵⁹ Additionally, the Chen group recently reported pH-responsive NIR-PCs consisting of imidazole-anion-fused perylene diimide chromophores (PDII⁻).⁶⁰ Notably, the PDII⁻/Cu dual-catalyzed photoinduced atom transfer radical polymerization (ATRP) can proceed smoothly ($\lambda_{\text{ex}} = 730$ nm) even when the vessels are covered by paper or pig skin, demonstrating the deep penetration capabilities of NIR photons.

Cyanine dyes, characterized by their conjugated polymethine chains flanked by heterocyclic rings, are renowned for their broad absorption spectrum extending from the visible to the NIR region. These dyes have found versatile applications across various fields, including NIR fluorescent imaging,⁶¹ oxygen photosensitization in PDT,⁶² and NIR photoredox catalysis. Their unique structure and extensive conjugation allow for significant versatility and effectiveness in these applications. A notable example of cyanine dye application is the work of Kütahya and co-workers, who employed the zwitterionic cyanine derivative (Cy791) as an NIR photoinitiator. This derivative, when irradiated with a 790 nm LED, proved effective for ATRP of methyl methacrylate (MMA)⁶³ and also Cu-catalyzed click reactions.⁶⁴ Further advancements were made in 2021 by the Goddard group, who demonstrated the multifaceted capabilities of Cy746.⁶⁵ This dye was shown to engage in oxidative quenching of heteroatom-containing substrates, reductive quenching of Umemoto's reagent, and energy-transfer processes, effectively generating reactive oxygen species. Their group's continued efforts in developing new cyanine-based NIR-PCs revealed that the amino-substituted cyanine dye (Cy637) significantly accelerates oxidative aza-Henry reactions, while a variant with an extended conjugated system (Cy997) exhibits enhanced stability under reducing conditions and proficiency in catalyzing trifluoromethylation of alkenes.⁶⁶ In addition to cyanine dyes, the Goddard group also explored the potential of squaraine derivatives (Sq) in NIR photocatalysis. Unlike cyanine dyes, squaraine dyes tend to participate predominantly in electron transfer photoredox processes, offering an alternative mechanism to the typically observed energy transfer in cyanine systems.⁶⁷ Complementing these developments, the Cheng group established a ketocyanine-type dye as a universal activator for a variety of reversible addition-fragmentation chain transfer (RAFT) polymerization. These polymerizations, activated by NIR LED light ($\lambda_{\text{ex}} = 810$ nm), underscore the expanding versatility and utility of cyanine and related dyes in advanced photoredox applications.⁶⁸

Porphyrinoids

Porphyrinoids, particularly aromatic porphyrins and phthalocyanines, along with their metal complexes, are distinguished from other organic dyes due to their exceptional optical and chemical properties (Figure 1C). Characterized by their robust aromatic structures, these compounds are known for their prominent Soret band at around 420 nm, making them traditionally favored as photoredox catalysts for reactions under blue and green light irradiation.^{69,70} A notable study by Gryko and

colleagues highlighted that base-free porphyrins are capable of promoting red-light-induced arylation of heterohydrocarbons through oxidative quenching. Additionally, they demonstrated that these compounds could also facilitate thiol-yne reactions and decarboxylative alkynylation via reductive quenching, showcasing the adaptability of porphyrins in engaging with different photoredox mechanisms.⁷¹ In pursuit of extending the light absorption range of porphyrins into the NIR region, the Derkson group made significant strides by modifying the porphyrin scaffold. They introduced a thiophene ring to the structure resulting in a red shift of the absorption band to 696 nm.⁷² This structural alteration has effectively expanded the utility of porphyrins, enabling them to act as photocatalysts for facilitating dehalogenation reactions under mild NIR irradiation ($\lambda_{\text{ex}} > 645$ nm).

The modification of porphyrinoid scaffolds extends beyond altering peripheral substituents. A significant avenue for enhancing their electronic structures and optical activities involves the introduction of main-group elements⁷³ or metals⁷⁴ as the central atom. This approach has led to a wide array of porphyrinoids with varied and improved functionalities, especially in terms of NIR photocatalysis. Silicon phthalocyanines are one such example, demonstrating high optical stability and the ability to promote photooxidative reactions under minimal catalyst loadings (in the ppb range) when irradiated at 630 nm.⁷⁵ Similarly, the Shibata group reported trifluorothoxy-coated B-subphthalocyanine (TFEO-SubPc), a catalyst that efficiently drives the trifluoromethylation of unsaturated hydrocarbons with good yields.⁷⁶

On the other hand, the potential of metal-centered porphyrinoids as NIR-PCs has been increasingly realized. Ouyang and colleagues reported Mg^{II} -chlorin, which catalyzed the photooxidative hydroxylation of organoboron compounds under LED irradiation.⁷⁷ In 2022, the MacMillan group introduced a novel proximity labeling strategy using a red-light-excited Sn^{IV} -chlorin, catalyzing the reduction of aryl azides to generate aminyl radicals, effective both *in vitro* and *in cellulo*.⁷⁸ Expanding the spectrum of NIR-responsive photocatalysts, Boyer and co-workers utilized aluminum phthalocyanine ($\lambda_{\text{max}} = 679$ nm) and aluminum naphthalocyanine ($\lambda_{\text{max}} = 783$ nm) for controlled RAFT polymerization under deep-red to NIR light.⁷⁹ Furthermore, the Furuyama group reported that ruthenium phthalocyanine complexes exhibited good compatibility with functional groups in the red-light-mediated chlorotrifluoromethylation reactions.⁸⁰ In the past decade, zinc phthalocyanines have also emerged as efficient photocatalysts promoting a variety of reactions including perfluoroalkylation reactions of (hetero)aromatics and sulfides under red light ($\lambda_{\text{ex}} = 635$ nm),⁸¹ cross-dehydrogenative coupling under NIR LED light ($\lambda_{\text{ex}} = 810$ nm),^{82,83} and RAFT polymerizations with NIR irradiation ($\lambda_{\text{ex}} = 730$ nm).⁸⁴

Metal polypyridyl complexes

Metal polypyridyl complexes represent a unique class of photocatalysts in the realm of organic photocatalysis, particularly because of their rich photophysical and redox chemistry (Figure 1D). In 2020, the Rovis group made a significant contribution to this field by reporting several Os polypyridyl complexes as effective NIR-PCs. Because of the strong spin-orbit coupling effect of the Os^{II} center, these Os complexes exhibit $\text{S}_0 \rightarrow \text{T}_1$ excitation in the deep-red and NIR regions (660–800 nm). This property allows them to effectively drive a variety of photoredox processes, including photopolymerization and metallaphotoredox reactions under NIR irradiation.⁸⁵ The versatility of Os polypyridyl complexes was further enhanced by the Rovis group through strategic modification of the ligand scaffold and electron density.⁸⁶ They successfully demonstrated a dual-nickel/[Os(phen)₃](PF₆)₂-catalyzed C–N cross-coupling of aryl

bromides with amine-based nucleophiles upon irradiation at 660 nm.⁸⁷ This Os photocatalyst was also shown to activate aryl azides and aryl(trifluoromethyl) diazos into nitrenes and carbenes, respectively, facilitating photocatalytic proximity labeling—a technique of growing interest for its potential in various chemical and biological applications.^{88,89} In addition, Landais and co-workers employed another variant, Os(bptpy)₂(PF₆)₂, as a catalyst to realize the decarboxylation of oxa-mic acids under deep-red conditions, highlighting the broad potential of Os^{II} poly-pyridyl complexes in facilitating various chemical transformations under NIR light.⁹⁰

Moreover, ruthenium polypyridyl complexes, such as [Ru(bpy)₃]²⁺ and [Ru(tpy)₂]²⁺, are well established in the domain of visible photoredox catalysis for their broad absorption band around 400–500 nm.⁹¹ The versatility and effectiveness of these complexes have led to their widespread adoption in various photocatalytic applications. Aiming to extend the capabilities of these ruthenium complexes, the Kurth group undertook modifications on [Ru(Tolyltpy)₂]²⁺. By introducing a central pyrimidine ring, they achieved red-shifted emission ($\lambda_{\text{em}} = 703$ nm) and prolonged excited-state lifetime ($\tau = 8.8 \pm 1$ ns). These modifications resulted in new Ru complexes with enhanced photostability and higher quantum yields. Remarkably, the modified complexes exhibit the ability to promote water reduction under red light irradiation.⁹²

In parallel, dirhodium complexes have garnered attention as promising NIR-PCs due to their panchromatic-light absorption and inherent stability in both water and air. The Turro group contributed to this field by developing Rh₂(II,II) dimers bridged with either symmetrical⁹³ or asymmetrical⁹⁴ ligands. These dimers are characterized by short Rh–Rh bonds, which elevate the energy of the Rh₂(σ*) orbital, leading to relatively long-lived ³ML-LCT (metal/ligand-to-ligand charge transfer) excited states. Such structural and electronic properties enable these dirhodium complexes to act effectively as NIR-PCs, particularly noted for their role in producing H₂ in acidic solutions ($\lambda_{\text{ex}} = 670$ or 735 nm).^{93,94} Moreover, when these dirhodium complexes are anchored onto a NiO photocathode, they perform dual functions as both the photosensitizer and catalytic center. This integration facilitates H₂ production under red light irradiation ($\lambda_{\text{ex}} = 655$ nm), effectively reducing energy loss typically associated with additional intermolecular charge transfer steps.⁹⁵ In addition, the iron(I) dimer [CpFe(CO)₂]₂ was reported to catalyze the iodoperfluoroalkylation of alkenes under NIR light ($\lambda_{\text{ex}} = 730$ nm) excitation. This process involves NIR-light-induced Fe–Fe bond homolysis to generate the metalloradical, which engages with perfluoroiodides to generate a perfluoroalkyl radical via a halogen-atom transfer process.⁹⁶

TTA-UC

The inherent limitation of conventional NIR-PCs lies in the low energy of NIR light, which may not suffice to drive certain chemically demanding transformations effectively.⁹⁷ To overcome this challenge, multiphoton excitation strategies, such as TTA-UC, have been developed.⁹⁸ By enabling the combination of energy from multiple photons within each catalytic turnover, TTA-UC facilitates the occurrence of thermodynamically challenging reactions under the irradiation of low-energy photons. This method essentially allows for the effective utilization of NIR photons, which are individually insufficient in energy, by accumulating their energy through a process of annihilation of triplet excited states. As a result, higher-energy singlet states are generated that are capable of initiating or driving reactions that single NIR photons cannot.⁹⁹

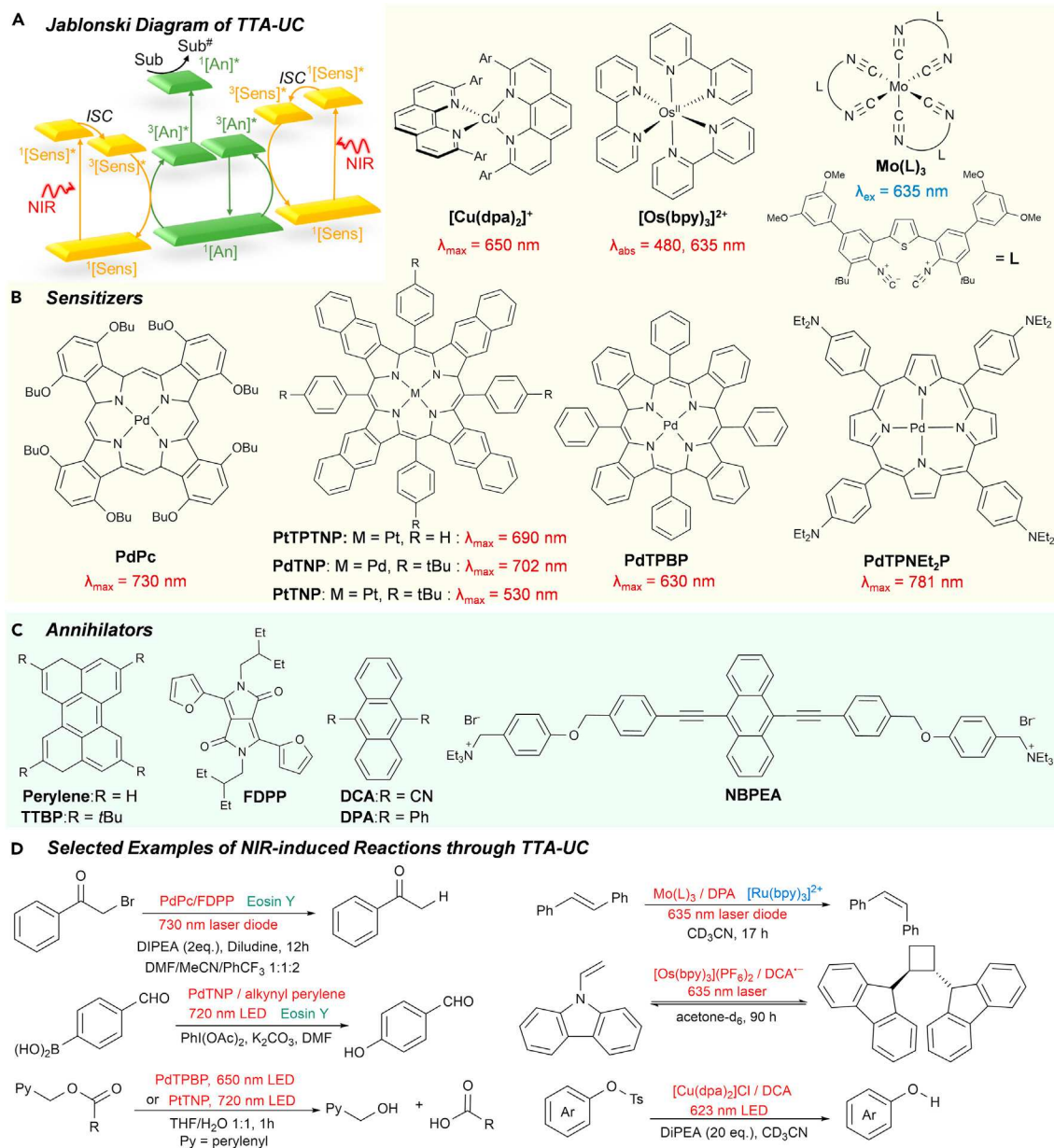


Figure 2. Schematic illustrations of TTA-UC pathways and selected examples of TTA-UC photocatalysis

(A) Jablonski diagram of TTA-UC.

(B) Sensitizers.

(C) Annihilators.

(D) Selected examples of NIR-induced reactions through TTA-UC.

UC is a nonlinear optical process characterized by the absorption of two or more low-energy photons and the subsequent emission of one higher-energy photon.¹⁰⁰ This process is inherently limited by quantum yield considerations, with the UC quantum yield (Φ_{UC}) theoretically restricted to less than 50%. The anti-Stokes shift (ΔE_{UC}) represents the energy difference between the absorbed low-energy photons and the emitted high-energy photon. TTA-UC is a specific UC mechanism that typically involves five key steps (Figure 2A). (1) The sensitizer (Sen) absorbs an NIR photon to generate its singlet excited state ($^1[Sen]^*$). (2) The $^1[Sen]^*$ undergoes intersystem

crossing (ISC) to form the corresponding long-lived triplet state ($^3[\text{Sen}]^*$). (3) The $^3[\text{Sen}]^*$ transfers its energy to the annihilator (An), resulting in the formation of the triplet excited state of the An ($^3[\text{An}]^*$). (4) Two $^3[\text{An}]^*$ species undergo TTA, leading to the formation of a singlet ground state and a singlet excited state of Ans ($^1[\text{An}]$ and $^1[\text{An}]^*$, respectively). (5) The high-energy $^1[\text{An}]^*$ decays into its ground state, accompanied by energy transfer or electron transfer processes with a conventional photocatalyst or substrate.

Achieving efficient TTA-UC requires careful consideration of several fundamental aspects. The ideal photosensitizer should exhibit intense light absorption, high ISC efficiency, and long triplet lifetime, while the ideal An should possess a high fluorescence quantum yield. There needs to be a specific energy relationship between the components, specifically, $E(^3[\text{Sen}]^*) > E(^3[\text{An}]^*)$ and $2E(^3[\text{An}]^*) > E(^1[\text{An}]^*) > E(^3[\text{Sen}]^*)$, to facilitate the effective transfer and annihilation of triplet energy. Moreover, the TTA pair must be spatially oriented to allow for Dexter energy transfer mechanisms, typically with a distance limitation of around 10 Å to ensure efficient energy transfer. Understanding and optimizing these parameters are critical in developing TTA-UC systems that effectively harness low-energy NIR photons for photocatalysis.

In 2019, Rovis, Campos, and co-workers reported NIR-irradiated photocatalysis following TTA-UC.¹⁰¹ They introduced a system employing Pd^{II}-octabutoxyphthalocyanine (PdPc) as the photosensitizer and furanyldiketopyrrolopyrrole (FDPP) as the An, achieving a remarkable NIR (730 nm) to orange (530 nm) TTA-UC with an Φ_{UC} of 3.2%. This TTA-UC system was successfully adapted to rose-bengal-mediated amine oxidation and eosin-Y-catalyzed hydrodehalogenation (Figure 2D) and radical cyclization reactions under NIR light excitation. Further expanding the potential of TTA-UC, the authors developed another NIR-to-blue Sen/An pair consisting of Pt^{II}-tetraphenyl-tetranaphthoporphyrin (PtTPTNP) and tetrakis(tert-butyl)perylene (TTBP). This pair achieved an Φ_{UC} of 2.0% and an anti-Stokes shift of approximately 1.0 eV. Demonstrating its versatility, this Sen/An pair was used for various reactions, including [2+2] cyclization reaction catalyzed by $[\text{Ru}(\text{bpy})_3]^{2+}$, vinyl azide cyclization, and the radical polymerization of MMA, all under the irradiation of an NIR diode.

In 2020, the Han group reported another NIR-to-green TTA-UC pair of Pd^{II}-tetraphenyl-tetranaphthoporphyrin (PdTNP) photosensitizer and perylene Ans.⁹⁷ The authors systematically explored their excited states by chemically modifying perylene Ans and successfully tuned the TTA-UC from an endothermic process to an exothermic one. This adjustment significantly enhanced the efficiency and practicality of TTA-UC in photocatalytic applications. With illumination under 720 nm light, the pair of PdTNP and bis(arylalkynyl)perylene exhibited a relatively high TTA-UC efficiency ($\Phi_{\text{UC}} = 14.1\%$), which enabled the eosin-Y-catalyzed photooxidation of arylboronic acid (Figure 2D). Furthermore, they discovered that excitation of the Sen tetraphenyltetrabenzoporphine palladium (PdTPBP) using 656 nm LEDs led to the generation of a high-energy excited state of perylene through TTA-UC. This state was capable of catalyzing the photoreduction of aryl halides even in the absence of electron sacrificial reagents.¹⁰² In parallel, Li and co-workers applied a red-light-illuminated TTA pair of Pd^{II}-5,10,15,20-tetra(N,N-diethylaniline)porphyrin (PdTPN₂P) and perylene to achieve selective degradation of oxidized lignin models.¹⁰³ The same group also introduced a TTA-mediated photolysis strategy in which the An was linked to a drug molecule via a photolabile chain.¹⁰⁴ Using PtTNP and PdTPBP as deep-red (650 nm) and NIR (720 nm) Sens, respectively, photoremoveable protecting groups such as BODIPY and perylene were activated via TTA-UC, facilitating the release of the drug by cleaving the photolabile linkage.

(Figure 2D). Moreover, PtTPBP^{105,106} and [Os(bptpy)₂]²⁺¹⁰⁷ have been reported as effective NIR-PCs to facilitate photolysis reactions of BODIPY-based prodrugs through UC-like processes, further expanding the applicability of TTA-UC in pharmaceutical contexts.

The Wenger group has introduced a novel family of photoactive compounds comprising Mo(0) complexes with diisocyanide chelate ligands.¹⁰⁸ Through meticulous ligand modification aimed at adjusting the bite angles and extending π -conjugation, they successfully obtained the deep-red luminescent Mo(0) complex, denoted as Mo(L)₃.¹⁰⁹ This complex was demonstrated to sensitize red (635 nm)-to-blue (430 nm) UC using 9,10-diphenylanthracene (DPA) as the An. The generated blue output light was then effectively harnessed by [Ru(bpy)₃]²⁺ to drive the photoisomerization reaction of stilbene in a separate reaction vessel (Figure 2D). More recently, the Wenger group reported another new bimolecular red-to-blue TTA-UC system comprised of [Os(bpy)₃]²⁺ and 9,10-dicyanoanthracene (DCA).¹¹⁰ This system was successfully employed in facilitating various photooxidative transformations, including the isomerization of stilbene, a [2+2] cycloaddition (Figure 2D), a Newman-Kwart rearrangement, and an aryl ether-to-ester rearrangement.

Beyond organometallic complexes, colloidal nanocrystals have emerged as a promising alternative for NIR UC to initiate various photocatalytic reactions. Wu and colleagues contributed to this expanding field by reporting an NIR-to-yellow TTA-UC pair consisting of Zn-doped CuInSe₂ nanocrystals and rubrene.¹¹¹ The Zn-doped CuInSe₂ nanocrystals act as efficient photosensitizers, absorbing NIR light and transferring energy to rubrene, the An. This pair could catalyze reductive dehalogenation, amine oxidation, cross-coupling, and polymerization reactions.

Several recent studies have indicated the potential of combining NIR-responsive TTA pairs with photocatalytic water-splitting cells to extend the optical spectral utilization of the photoanodes, consequently leading to improved quantum yields and more efficient photocatalytic H₂ production. For example, Moon and co-workers pioneered this approach by modifying a Mo:BiVO₄ photoanode with a luminescent back reflector polymer film containing a red-to-blue TTA-UC couple, meso-PdTPBP and perylene.¹¹² This modification effectively expanded the photoanode's light absorption spectrum, enhancing its overall photocatalytic activity and H₂ production efficiency.

Similarly, Li and co-workers applied this concept further by integrating a semiconductor Cd_{0.5}Zn_{0.5}S with a red-to-cyan TTA-UC micelle composed of PdTPBP and 9,10-bis(phenylethynyl)anthracene ammonium salt (NBPEA).¹¹³ This innovative combination leveraged the unique properties of both the semiconductor and the TTA-UC pair, resulting in a synergistic effect that significantly boosted the photocatalytic H₂ production. Additionally, the Li group developed a strategy to enhance the efficiency of TTA-UC in water-splitting cells by attaching the DPA An to a dendritic molecular wire. This design effectively prevents Förster resonance energy transfer-type back energy transfer from the upconverted An to the Sen (PdTPBP), thus showing substantial promotion of the photocatalytic H₂ production.¹¹⁴

In 2022, Wenger and colleagues introduced a cooperative catalytic strategy based on a biphotonic excitation mechanism.¹¹⁵ This pioneering approach enables the harnessing of red light (623 nm LED) to facilitate challenging dehalogenation and

detosylation reactions (Figure 2D). The heart of this innovative strategy is dual photocatalysis, which employs a Cu¹-bis(α -diimine) complex, specifically [Cu(dpa)₂]Cl, in combination with *in-situ*-generated 9,10-dicyanoanthracenyl radical anion (DCA^{•-}), in the presence of a sacrificial electron donor, creating a system capable of effectively utilizing red light to drive the targeted reactions.

TPA

In addition to TTA-UC, TPA is another nonlinear optical phenomenon. Initially predicted by Göppert-Mayer in 1929^{116,117} and experimentally confirmed by Garrett and co-workers in 1961,¹¹⁸ TPA has since become a fundamental concept in the field of photophysics and photochemistry. Contrary to OPA, TPA is characterized by the simultaneous absorption of two photons, which occurs in two primary steps (Figure 3A). Initially, one photon is absorbed by the chromophore, leading to the formation of a short-lived nonresonant excited state, referred to as the “virtual state.” Crucially, for the continuation of the TPA process, a second photon must arrive within the attosecond timescale to further excite the virtual state to a higher-energy singlet excited state. A notable aspect of TPA is that the fluorescence intensity induced by this process increases with the square of the excitation light intensity, indicating its nonlinear nature.¹¹⁹ Because of the small TPA cross-sections of most molecules, an excitation light source of high power density is usually required for TPA studies, which started to take off after the advent of subpicosecond-pulsed lasers in the 1990s.¹²⁰ Since then, TPA has been harnessed in a multitude of applications ranging from bioimaging^{121–123} and microscopy^{124,125} to 3D data storage¹²⁶ and PDT.^{127–129}

Recent studies have demonstrated that TPA can also be effectively induced using more economical light sources, such as LEDs or Xe lamps,^{130–134} thus expanding its potential in various photocatalytic applications. In the context of NIR photocatalysis, molecular engineering strategies have been employed to develop and enhance TPA photocatalytic systems, including metal-organic frameworks (MOFs) and molecular TPA photocatalysts, which will be summarized in this section.

MOF-based TPA photocatalysts

MOFs are porous crystalline materials renowned for their structural versatility, chemical flexibility, and designability. These attributes make MOFs particularly intriguing for photocatalytic applications. Recently, photon-responsive MOFs have garnered significant interest because their properties can be readily tuned and activated by light irradiation, making them suitable for a variety of light-driven processes. One effective approach for endowing MOFs with NIR two-photon harvesting capabilities involves the incorporation of photoactive molecules into their structures (Figure 3B). By attaching these molecules, typically known for their strong NIR absorption and efficient TPA properties, to the MOF, the resultant materials can effectively harness NIR light for photocatalytic applications.

Chen, Qian, and co-workers made a notable contribution to the field of MOF-based photocatalysis by ingeniously incorporating a zwitterionic photoactive pyridinium linker into the MOF ZJU-56-0.2 using a multivariate strategy. This strategic modification endowed the MOF with the capability of TPA under NIR irradiation, significantly broadening its application in photocatalysis.¹³⁵ The Duan group took advantage of this enhanced MOF to achieve photocatalytic C–N and C–O oxidative coupling reactions via a TPA process, specifically under the irradiation of 660 nm LEDs (Figure 3E).¹³⁰ Interestingly, the TPA ability of ZJU-56-0.2 was found to increase with

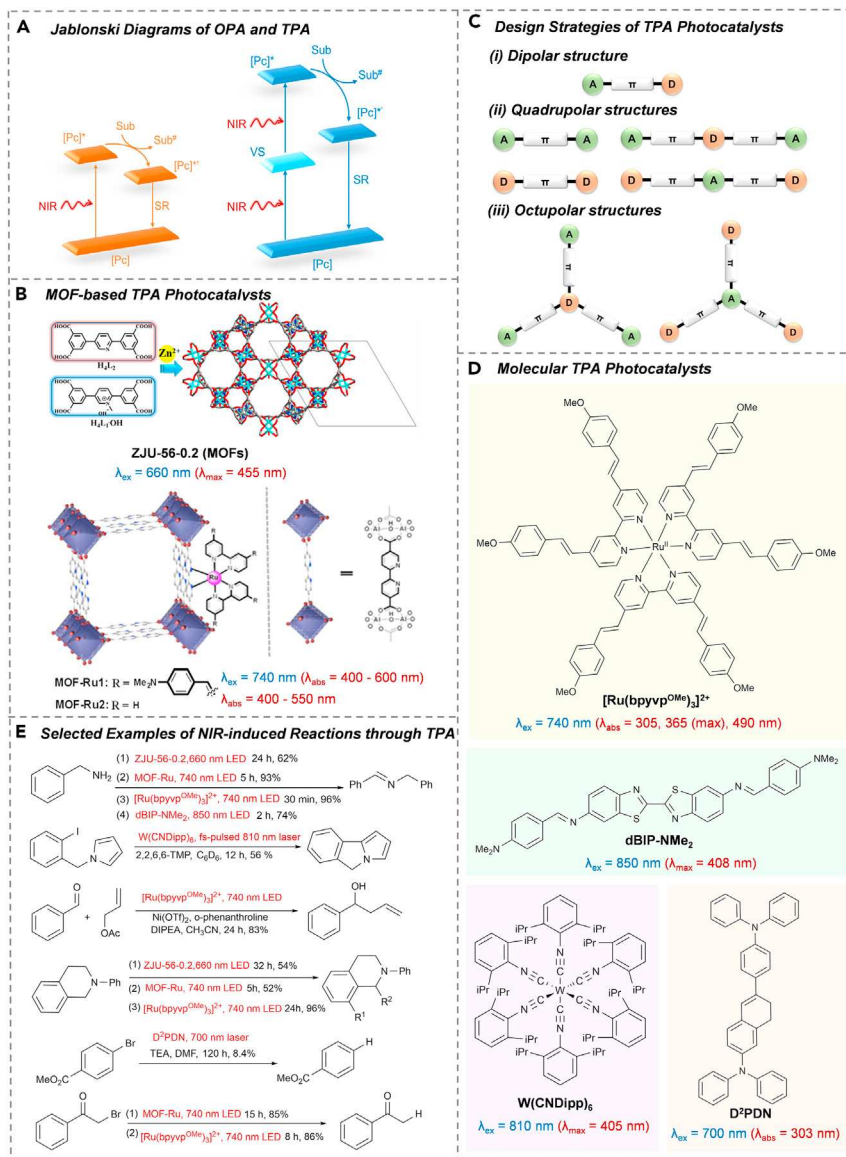


Figure 3. Schematic illustrations of OPA and TPA pathways and selected examples of TPA photocatalysis

(A) Jablonski diagrams of OPA and TPA.
 (B) MOF-based TPA photocatalysts.
 (C) Design strategies of TPA photocatalysts.
 (D) Molecular TPA photocatalysts.
 (E) Selected examples of NIR-induced reactions following the TPA mechanism.

the proportion of pyridinium salt ligands within the framework. This correlation suggests that the photocatalytic efficiency of the MOF can be systematically improved by adjusting the amount of photoactive ligands.

In 2020, Chao, Gasser, and their colleagues discovered that certain ruthenium complexes with π -extended polypyridyl ligands could act as effective two-photon PDT reagents under NIR light irradiation.¹³⁶ Building on this finding, the Sun group integrated analogous ruthenium polypyridine complexes into MOFs to create a new class of MOF-based TPA photocatalysts.¹³² Under the irradiation of 740 nm LEDs,

the resulting MOF-Ru1 is capable of undergoing a TPA process, effectively harnessing NIR light to initiate various organic transformations, such as the $^1\text{O}_2$ -driven C-N coupling of benzylamines, various redox reactions, and ATRP (Figure 3E).

Molecular TPA photocatalysts

Unlike their MOF-based counterparts, molecular photocatalysts are characterized by their well-defined and readily tunable structures, making them particularly promising for homogeneous TPA photocatalysis. While the discovery of many TPA chromophores has been somewhat serendipitous, there are empirical design principles that guide the creation of competent TPA molecules. For instance, a large π -conjugated system can enhance the absorption of light and facilitate the delocalization of electrons across the molecule, contributing to its ability to absorb two photons simultaneously. Coplanarity in the structure is often sought to maximize the effectiveness of π -conjugation. Incorporating electron-donating and electron-accepting groups connected by π -conjugated bridges into the molecular structure can help to create a push-pull electronic environment (Figure 3C). This arrangement facilitates the movement of electrons and holes when the molecule absorbs photons, increasing the efficiency of the TPA process. Introducing centrosymmetric quadrupolar or branched octupolar structural motifs into the molecular design can enhance the molecule's optical and electronic properties, making it more effective in TPA processes. Symmetric structures, in particular, can lead to better alignment of energy levels and more efficient electronic transitions.¹²⁰

In 2017, Gray and co-workers discovered that homoleptic tungsten(0) arylisocyanide $\text{W}(\text{CNAr})_6$ exhibited an extremely large TPA cross-section ($\delta > 10^3$ GM)¹³⁷ and highly negative reduction potentials. When bulky 2,6-iPr-substituted arylisocyanides were employed to provide steric protection, the resulting $\text{W}(\text{CNDipp})_6$ complex (Figure 3D) showed a cross-section of 230 GM measured with femtosecond-pulsed 810 nm excitation. $\text{W}(\text{CNDipp})_6$ was able to drive the single-photon visible and two-photon NIR light-promoted photoreduction of aryl iodide (Figure 3E).¹³⁸

On the other hand, Ru^{II} polypyridyl complexes with extended π -conjugated ligands have garnered considerable attention as TPA PDT agents¹³⁹ and photoactivatable compounds¹⁴⁰ due to their unique photophysical properties. For instance, the Sun group recently reported that $[\text{Ru}(\text{bpyvp})_3]^{2+}$ ($\text{bpyvp} = 4,4'\text{-bisstyryl-2,2'-bipyridine}$) complexes (Figure 3D) featuring *trans*-styryl branches can act as competent TPA NIR-PCs capable of driving a range of energy transfer and photoredox reactions under 740 nm LED irradiation.¹³¹ This versatility underscores the potential of these complexes in various photocatalytic applications, including those requiring deep tissue penetration or minimally invasive procedures, as is often the case in biomedical applications. This work also demonstrates the feasibility of using economical and easily accessible LEDs for homogeneous TPA photocatalysis.

Compared to metal complexes, organic photocatalysts could be more cost effective and environmentally friendly, making them increasingly attractive for practical applications. In the pursuit of developing new metal-free photocatalysts with efficient TPA, the Sun group recently reported a series of benzothiazole-derived molecules (dBIPs).¹³⁴ These molecules were specifically engineered to include terminal electron-donating groups, which significantly improved their photocatalytic activity. This enhancement is likely due to the increased TPA cross-section and prolonged excited-state lifetime imparted by these modifications. A notable example from this series is a dBIP derivative substituted with a dimethylamino group (dBIP-NMe₂; Figure 3D). This modified molecule exhibits a TPA cross-section nearing

2,000 GM at 850 nm, representing a significant increase in TPA efficiency. As a result, dBIP-NMe₂ effectively catalyzes various O₂-involved energy transfer reactions under 850 nm LED irradiation. Similarly, by substituting dBIP with a methoxyl group (dBIP-OMe), the same group demonstrated its capability in catalyzing trifluoromethylated bifunctionalization of olefins without the need for sacrificial reagents under 740 nm LED irradiation.¹³³

Recently, the Abe group introduced electron-donating diphenylamino groups into the quadrupolar donor- π -donor system, resulting in a novel cyclic stilbene derivative (D²PDN; Figure 3D).¹⁴¹ This photosensitizer exhibited a TPA cross-section of \sim 170 GM at 700 nm and demonstrated its capability as a potent photocatalyst, particularly in catalyzing the reduction reaction of aryl bromides under 700 nm Ti-sapphire laser irradiation.

The introduction of dBIP, D²PDN, and other metal-free TPA compounds reflects a growing interest and ongoing innovation in the field of organic photocatalysis. As researchers continue to explore and understand the vast potential of TPA photocatalysis, the development of new, efficient, and environmentally friendly organic TPA photocatalysts is expected to accelerate. This burgeoning area of research holds great promise for advancing the capabilities and applications of photocatalysis, particularly as more sophisticated and effective metal-free TPA compounds are discovered and optimized for various light-driven processes.

OUTLOOK

This review highlights the various types of molecular NIR light-absorbing photocatalysts classified by their excitation mechanisms, including OPA, TTA-UC, and TPA. The potential for precise modulation of electronic structures and optical properties through molecular design cannot be overestimated, yet the path to practical and commercial applications of these technologies is lined with challenges.

Red-shifted OPA photocatalysts, while beneficial for long-wavelength absorption, often face trade-offs with reduced quantum yield and lower excited-state energy and redox power, limiting the scope of feasible reactions to be catalyzed. Additionally, the synthesis of molecular photocatalysts that absorb NIR light is usually complex and resource intensive. Future research may focus on developing more efficient and simpler synthetic routes, as well as exploring new systems to enhance quantum yields and reaction scopes.

On the other hand, the TTA-UC strategy overcomes the energy limitation of NIR photons by converting long-wavelength light into higher-lying excited states, which are possible for driving various photoreactions. Despite these benefits, TTA-UC systems fall short in terms of requiring an oxygen-free environment and face challenges with low quantum yields due to multiple energy transfer steps. Future efforts might involve designing more robust Sens and Ans, as well as innovative strategies to protect TTA-UC systems from oxygen quenching and to improve their overall quantum yields.

Finally, TPA photocatalysts offer exciting opportunities by allowing the simultaneous absorption of two NIR photons, thereby expanding the spectrum of usable excitation light. Although traditionally associated with intense lasers, recent reports suggest inexpensive NIR LEDs can also be employed as the light source for NIR light-driven photocatalysis following the TPA strategy. Nevertheless, the bottleneck for its

wide adoption in organic photocatalysis is the development of photocatalysts with adequate TPA cross-section and photocatalytic efficiency. Technological advancement in the accurate prediction and measurement of TPA cross-section is also crucial.

Despite significant progress in developing NIR-PCs, the journey toward wide-scale industrial and commercial use has just started. As NIR photocatalysis continues to evolve, it will undoubtedly find applications across various fields like organic synthesis, bioimaging, biomolecule labeling, and drug delivery. Selecting appropriate application scenarios and continuously improving the molecular design of NIR-PCs will be key to facilitating the commercialization of these scientific advancements.

ACKNOWLEDGMENTS

Y.S. is thankful for the support of the National Science Foundation (CHE-1955358) and the University of Cincinnati.

AUTHOR CONTRIBUTIONS

Conceptualization, Y.S.; writing – original draft, M.Z.; writing – review & editing, Y.S.

DECLARATION OF INTERESTS

The authors declare no competing interests.

REFERENCES

1. Narayanan, J.M.R., and Stephenson, C.R.J. (2011). Visible light photoredox catalysis: applications in organic synthesis. *Chem. Soc. Rev.* 40, 102–113. <https://doi.org/10.1039/B913880N>.
2. Tucker, J.W., and Stephenson, C.R.J. (2012). Shining light on photoredox catalysis: Theory and synthetic applications. *J. Org. Chem.* 77, 1617–1622. <https://doi.org/10.1021/jo202538x>.
3. Prier, C.K., Rankic, D.A., and MacMillan, D.W.C. (2013). Visible light photoredox catalysis with transition metal complexes: Applications in organic synthesis. *Chem. Rev.* 113, 5322–5363. <https://doi.org/10.1021/cr300503r>.
4. Twilton, J., Le, C., Zhang, P., Shaw, M.H., Evans, R.W., and MacMillan, D.W.C. (2017). The merger of transition metal and photocatalysis. *Nat. Rev. Chem.* 1, 0052. <https://doi.org/10.1038/s41570-017-0052>.
5. Arias-Rotondo, D.M., and McCusker, J.K. (2016). The photophysics of photoredox catalysis: a roadmap for catalyst design. *Chem. Soc. Rev.* 45, 5803–5820. <https://doi.org/10.1039/C6CS00526H>.
6. Kärkäs, M.D., Porco, J.A., and Stephenson, C.R.J. (2016). Photochemical approaches to complex chemotypes: Applications in natural product synthesis. *Chem. Rev.* 116, 9683–9747. <https://doi.org/10.1021/acs.chemrev.5b00760>.
7. Ryu, K.A., Kaszuba, C.M., Bissonnette, N.B., Oslund, R.C., and Fadeyi, O.O. (2021). Interrogating biological systems using visible-light-powered catalysis. *Nat. Rev. Chem.* 5, 322–337. <https://doi.org/10.1038/s41570-021-00265-6>.
8. Holder, A.A., Lilge, L., Browne, W.R., Lawrence, M.A.W., and Bullock, J.J.L. (2018). *Ruthenium Complexes: Photochemical and Biomedical Applications* (Wiley-VCH).
9. Wang, D., Marquard, S.L., Troian-Gautier, L., Sheridan, M.V., Sherman, B.D., Wang, Y., Eberhart, M.S., Farnum, B.H., Dares, C.J., and Meyer, T.J. (2018). Interfacial Deposition of Ru(II) bipyridine-dicarboxylate complexes by ligand substitution for applications in water oxidation catalysis. *J. Am. Chem. Soc.* 140, 719–726. <https://doi.org/10.1021/jacs.7b10809>.
10. Gueret, R., Poulard, L., Oshinowo, M., Chauvin, J., Dahmane, M., Dupeyre, G., Lainé, P.P., Fortage, J., and Collomb, M.-N. (2018). Challenging the $[\text{Ru}(\text{bpy})_3]^{2+}$ photosensitizer with a triazatriangulenium robust organic dye for visible-light-driven hydrogen production in water. *ACS Catal.* 8, 3792–3802. <https://doi.org/10.1021/acscatal.7b04000>.
11. Limburg, B., Bouwman, E., and Bonnet, S. (2016). Rate and stability of photocatalytic water oxidation using $[\text{Ru}(\text{bpy})_3]^{2+}$ as photosensitizer. *ACS Catal.* 6, 5273–5284. <https://doi.org/10.1021/acscatal.6b00107>.
12. Boutin, E., Merakeb, L., Ma, B., Boudy, B., Wang, M., Bonin, J., Anxolabéhère-Mallart, E., and Robert, M. (2020). Molecular catalysis of CO_2 reduction: recent advances and perspectives in electrochemical and light-driven processes with selected Fe, Ni and Co aza macrocyclic and polypyridine complexes. *Chem. Soc. Rev.* 49, 5772–5809. <https://doi.org/10.1039/DOCS00218F>.
13. Zhang, J. (2018). Conversion of lignin models by photoredox catalysis. *ChemSusChem* 11, 3071–3080. <https://doi.org/10.1002/cssc.201801370>.
14. O'Regan, B., and Grätzel, M. (1991). A low-cost, high-efficiency solar cell based on dye-sensitized colloidal TiO_2 films. *Nature* 353, 737–740. <https://doi.org/10.1038/353737a0>.
15. Wang, Q., Zakeeruddin, S.M., Nakeeruddin, M.K., Humphry-Baker, R., and Grätzel, M. (2006). Molecular wiring of nanocrystals: NCS-enhanced cross-surface charge transfer in self-assembled Ru-complex monolayer on mesoscopic oxide films. *J. Am. Chem. Soc.* 128, 4446–4452. <https://doi.org/10.1021/ja058616h>.
16. Bella, F., Gerbaldi, C., Barolo, C., and Grätzel, M. (2015). Aqueous dye-sensitized solar cells. *Chem. Soc. Rev.* 44, 3431–3473. <https://doi.org/10.1039/C4CS00456F>.
17. Núñez, M.E., and Barton, J.K. (2000). Probing DNA charge transport with metallointercalators. *Curr. Opin. Chem. Biol.* 4, 199–206. [https://doi.org/10.1016/S1367-5931\(99\)00075-7](https://doi.org/10.1016/S1367-5931(99)00075-7).
18. Cook, N.P., Torres, V., Jain, D., and Martí, A.A. (2011). Sensing amyloid- β aggregation using luminescent dipyridophenazine ruthenium(II) complexes. *J. Am. Chem. Soc.* 133, 11121–11123. <https://doi.org/10.1021/ja204656r>.
19. Zhang, R., and Yuan, J. (2020). Responsive metal complex probes for time-gated luminescence biosensing and imaging. *Acc. Chem. Res.* 53, 1316–1329. <https://doi.org/10.1021/acs.accounts.0c00172>.

20. Shum, J., Leung, P.K.-K., and Lo, K.K.-W. (2019). Luminescent ruthenium(II) polypyridine complexes for a wide variety of biomolecular and cellular applications. *Inorg. Chem.* 58, 2231–2247. <https://doi.org/10.1021/acs.inorgchem.8b02979>.

21. Shen, J., Rees, T.W., Ji, L., and Chao, H. (2021). Recent advances in ruthenium(II) and iridium(III) complexes containing nanosystems for cancer treatment and bioimaging. *Coord. Chem. Rev.* 443, 214016. <https://doi.org/10.1016/j.ccr.2021.214016>.

22. Mdilui, V., Diluzio, S., Lewis, J., Kowalewski, J.F., Connell, T.U., Yaron, D., Kowalewski, T., and Bernhard, S. (2020). High-throughput synthesis and screening of iridium(III) photocatalysts for the fast and chemoselective dehalogenation of aryl bromides. *ACS Catal.* 10, 6977–6987. <https://doi.org/10.1021/acscatal.0c02247>.

23. Shon, J.-H., Kim, D., Rathnayake, M.D., Sittel, S., Weaver, J., and Teets, T.S. (2021). Photoredox catalysis on unactivated substrates with strongly reducing iridium photosensitizers. *Chem. Sci.* 12, 4069–4078. <https://doi.org/10.1039/D0SC06306A>.

24. Tucker, J.W., and Stephenson, C.R.J. (2011). Tandem visible light-mediated radical cyclization–divinylcyclopropane rearrangement to tricyclic pyrrolidinones. *Org. Lett.* 13, 5468–5471. <https://doi.org/10.1021/o1202178t>.

25. Eisenhofer, A., Hioe, J., Gschwind, R.M., and König, B. (2017). Photocatalytic phenol–arene C–C and C–O cross-dehydrogenative coupling. *Eur. J. Org. Chem.* 2017, 2194–2204. <https://doi.org/10.1002/ejoc.201700211>.

26. Yang, Y., Tan, H., Cheng, B., Fan, J., Yu, J., and Ho, W. (2021). Near-infrared-responsive photocatalysts. *Small Methods* 5, e2001042. <https://doi.org/10.1002/smtd.202001042>.

27. Han, C., Kundu, B.K., Liang, Y., and Sun, Y. (2024). Near-infrared light-driven photocatalysis with an emphasis on two-photon excitation: Concepts, materials, and applications. *Adv. Mater.* 36, e2307759. <https://doi.org/10.1002/adma.202307759>.

28. Sellet, N., Cormier, M., and Goddard, J.-P. (2021). The dark side of photocatalysis: near-infrared photoredox catalysis for organic synthesis. *Org. Chem. Front.* 8, 6783–6790. <https://doi.org/10.1039/d1qo01476e>.

29. Schade, A.H., and Mei, L. (2023). Applications of red light photoredox catalysis in organic synthesis. *Org. Biomol. Chem.* 21, 2472–2485. <https://doi.org/10.1039/d3ob00107e>.

30. Le, C.C., Wismer, M.K., Shi, Z.-C., Zhang, R., Conway, D.V., Li, G., Vachal, P., Davies, I.W., and MacMillan, D.W.C. (2017). A general small-scale reactor to enable standardization and acceleration of photocatalytic reactions. *ACS Cent. Sci.* 3, 647–653. <https://doi.org/10.1021/acscentsci.7b00159>.

31. Gisbertz, S., Reischauer, S., and Pieber, B. (2020). Overcoming limitations in dual photoredox/nickel-catalysed C–N cross-couplings due to catalyst deactivation. *Nat. Catal.* 3, 611–620. <https://doi.org/10.1038/s41929-020-0473-6>.

32. Ash, C., Dubec, M., Donne, K., and Bashford, T. (2017). Effect of wavelength and beam width on penetration in light-tissue interaction using computational methods. *Laser Med. Sci.* 32, 1909–1918. <https://doi.org/10.1007/s10103-017-2317-4>.

33. Juzenas, P., Juzeniene, A., Kaalhus, O., Iani, V., and Moan, J. (2002). Noninvasive fluorescence excitation spectroscopy during application of 5-aminolevulinic acid *in vivo*. *Photochem. Photobiol. Sci.* 1, 745–748. <https://doi.org/10.1039/b203459j>.

34. Ruggiero, E., Alonso-de Castro, S., Habtemariam, A., and Salassa, L. (2016). Upconverting nanoparticles for the near infrared photoactivation of transition metal complexes: new opportunities and challenges in medicinal inorganic photochemistry. *Dalton Trans.* 45, 13012–13020. <https://doi.org/10.1039/C6DT01428C>.

35. Wang, L., Xu, X., Cheng, Q., Dou, S.X., and Du, Y. (2021). Near-infrared-driven photocatalysts: Design, construction, and applications. *Small* 17, 1904107. <https://doi.org/10.1002/smll.201904107>.

36. Kaim, W. (2011). Concepts for metal complex chromophores absorbing in the near infrared. *Coord. Chem. Rev.* 255, 2503–2513. <https://doi.org/10.1016/j.ccr.2011.01.014>.

37. Wu, S., Blinco, J.P., and Barner-Kowollik, C. (2017). Near-Infrared Photoinduced Reactions Assisted by Upconverting Nanoparticles. *Chem. Eur. J.* 23, 8325–8332. <https://doi.org/10.1002/chem.201700658>.

38. Connell, T.U. (2022). The forgotten reagent of photoredox catalysis. *Dalton Trans.* 51, 13176–13188. <https://doi.org/10.1039/D2DT01491B>.

39. Bergmann, K., and O’Konski, C.T. (1963). A spectroscopic study of methylene blue monomer, dimer, and complexes with montmorillonite. *J. Phys. Chem.* 67, 2169–2177. <https://doi.org/10.1021/j100804a048>.

40. Cocquet, G., Ferroud, C., and Guy, A. (2000). A mild and efficient procedure for ring-opening reactions of piperidine and pyrrolidine derivatives by single electron transfer photooxidation. *Tetrahedron* 56, 2975–2984. [https://doi.org/10.1016/S0040-4020\(00\)00048-X](https://doi.org/10.1016/S0040-4020(00)00048-X).

41. Cocquet, G., Ferroud, C., Simon, P., and Taberna, P.-L. (2000). Single electron transfer photoinduced oxidation of piperidine and pyrrolidine derivatives to the corresponding lactams. *J. Chem. Soc., Perkin Trans. 2* 2000, 1147–1153. <https://doi.org/10.1039/b001036g>.

42. Watanabe, K., Terao, N., Kii, I., Nakagawa, R., Niwa, T., and Hosoya, T. (2020). Indolizines enabling rapid uncaging of alcohols and carboxylic acids by red light-induced photooxidation. *Org. Lett.* 22, 5434–5438. <https://doi.org/10.1021/acs.orglett.0c01799>.

43. Goulet-Hanssens, A., Rietze, C., Titov, E., Abdullah, L., Grubert, L., Saalfrank, P., and Hecht, S. (2018). Hole catalysis as a general mechanism for efficient and wavelength-independent Z → E azobenzene isomerization. *Chem* 4, 1740–1755. <https://doi.org/10.1016/j.chempr.2018.06.002>.

44. Lancel, M., Gomez, C., Port, M., and Amara, Z. (2021). Performances of homogeneous and heterogenized methylene blue on silica under red light in batch and continuous flow photochemical reactors. *Front. Chem. Eng.* 3, <https://doi.org/10.3389/fceng.2021.752364>.

45. Zhao, Z., Li, J., Yuan, W., Cheng, D., Ma, S., Li, Y.F., Shi, Z.J., and Hu, K. (2024). Nature-inspired photocatalytic azo bond cleavage with red light. *J. Am. Chem. Soc.* 146, 1364–1373. <https://doi.org/10.1021/jacs.3c09837>.

46. Laursen, B.W., and Krebs, F.C. (2000). Synthesis of a triazatriangulenium salt. *Angew. Chem. Int. Ed.* 39, 3432–3434. [https://doi.org/10.1002/1521-3773\(20001002\)39:19<3432::Aid-anie3432>3.0.co;2-s](https://doi.org/10.1002/1521-3773(20001002)39:19<3432::Aid-anie3432>3.0.co;2-s).

47. Sørensen, T.J., Nielsen, M.F., and Laursen, B.W. (2014). Synthesis and stability of N,N'-dimethyl-1,13-dimethoxyquinacridinium (DMQA⁺): A [4]helicene with multiple redox states. *ChemPlusChem* 79, 1030–1035. <https://doi.org/10.1002/cplu.201402058>.

48. Delgado, I.H., Pascal, S., Wallabregue, A., Duwald, R., Besnard, C., Guénée, L., Nançoz, C., Vauthey, E., Tovar, R.C., Lunkley, J.L., et al. (2016). Functionalized cationic [4]helicenes with unique tuning of absorption, fluorescence and chiroptical properties up to the far-red range. *Chem. Sci.* 7, 4685–4693. <https://doi.org/10.1039/c6sc00614k>.

49. Duwald, R., Pascal, S., Bosson, J., Grass, S., Besnard, C., Bürgi, T., and Lacour, J. (2017). Enantiospecific elongation of cationic helicenes by electrophilic functionalization at terminal ends. *Chem.* 23, 13596–13601. <https://doi.org/10.1002/chem.201703441>.

50. Gianetti, T., and Mei, L. (2020). Helical carbenium ion-based organic photoredox catalyst: A versatile and sustainable option in red-light-induced reactions. *Synlett* 32, 337–343. <https://doi.org/10.1055/s-0040-1705942>.

51. Mei, L., Veleta, J.M., and Gianetti, T.L. (2020). Helical carbenium ion: A versatile organic photoredox catalyst for red-light-mediated reactions. *J. Am. Chem. Soc.* 142, 12056–12061. <https://doi.org/10.1021/jacs.0c05507>.

52. Mei, L., Moutet, J., Stull, S.M., and Gianetti, T.L. (2021). Synthesis of CF₃-containing spirocyclic indolines via a red-light-mediated trifluoromethylation/dearomatization cascade. *J. Org. Chem.* 86, 10640–10653. <https://doi.org/10.1021/acs.joc.1c01313>.

53. Gianetti, T.L., Stull, S.M., and Mei, L. (2021). Red-light-induced N,N'-dipropyl-1,13-dimethoxyquinacridinium-catalyzed [3+2] cycloaddition of cyclopropylamines with alkenes or alkynes. *Synlett* 33, 1194–1198. <https://doi.org/10.1055/a-1665-9220>.

54. Hari, D.P., and König, B. (2014). Synthetic applications of eosin Y in photoredox catalysis. *Chem. Commun.* 50, 6688–6699. <https://doi.org/10.1039/c4cc00751d>.

55. Tanioka, M., Kuromiya, A., Ueda, R., Obata, T., Muranaka, A., Uchiyama, M., and Kamino, S. (2022). Bridged eosin Y: a visible and near-infrared photoredox catalyst. *Chem. Commun.* 58, 7825–7828. <https://doi.org/10.1039/d2cc02907c>.

56. De Bonfils, P., Péault, L., Nun, P., and Coeffard, V. (2021). State of the art of bodipy-based photocatalysts in organic synthesis. *Eur. J. Org. Chem.* 2021, 1809–1824. <https://doi.org/10.1002/ejoc.202001446>.

57. Kamkaew, A., Lim, S.H., Lee, H.B., Kiew, L.V., Chung, L.Y., and Burgess, K. (2013). BODIPY dyes in photodynamic therapy. *Chem. Soc. Rev.* 42, 77–88. <https://doi.org/10.1039/c2cs35216h>.

58. Huang, L., Li, Z., Zhao, Y., Zhang, Y., Wu, S., Zhao, J., and Han, G. (2016). Ultralow-power near infrared lamp light operable targeted organic nanoparticle photodynamic therapy. *J. Am. Chem. Soc.* 138, 14586–14591. <https://doi.org/10.1021/jacs.6b05390>.

59. Zeng, L., Wang, Z., Zhang, T., and Duan, C. (2022). Direct utilization of near-infrared light for photooxidation with a metal-free photocatalyst. *Molecules* 27, 4047. <https://doi.org/10.3390/molecules27134047>.

60. Ti, Q., Fang, L., Zhao, W., Bai, L., Zhao, H., Ba, X., and Chen, W. (2023). Near-infrared light and acid/base dual-regulated polymerization utilizing imidazole-anion-fused perylene diimides as photocatalysts. *J. Am. Chem. Soc.* 145, 26160–26168. <https://doi.org/10.1021/jacs.3c08503>.

61. Sun, W., Guo, S., Hu, C., Fan, J., and Peng, X. (2016). Recent development of chemosensors based on cyanine platforms. *Chem. Rev.* 116, 7768–7817. <https://doi.org/10.1021/acs.chemrev.6b00001>.

62. Lange, N., Szlasa, W., Saczko, J., and Chwiłkowska, A. (2021). Potential of cyanine derived dyes in photodynamic therapy. *Pharmaceutics* 13, 818. <https://doi.org/10.3390/pharmaceutics13060818>.

63. Kütahya, C., Schmitz, C., Strehmel, V., Yagci, Y., and Strehmel, B. (2018). Near-infrared sensitized photoinduced atom-transfer radical polymerization (ATRP) with a copper(II) catalyst concentration in the ppm range. *Angew. Chem. Int. Ed.* 57, 7898–7902. <https://doi.org/10.1002/anie.201802964>.

64. Kütahya, C., Yagci, Y., and Strehmel, B. (2019). Near-infrared photoinduced copper-catalyzed azide-alkyne click chemistry with a cyanine comprising a barbiturate group. *ChemPhotoChem* 3, 1180–1186. <https://doi.org/10.1002/cptc.201900012>.

65. Obah Kosso, A.R., Sellet, N., Baralle, A., Cormier, M., and Goddard, J.P. (2021). Cyanine-based near infra-red organic photoredox catalysis. *Chem. Sci.* 12, 6964–6968. <https://doi.org/10.1039/d1sc00998b>.

66. Sellet, N., Clement-Comoy, L., Elhabiri, M., Cormier, M., and Goddard, J.P. (2023). Second generation of near-infrared cyanine-based photocatalysts for faster organic transformations. *Chem. Eur. J.* 29, e202302353. <https://doi.org/10.1002/chem.202302353>.

67. Sellet, N., Sebbat, M., Elhabiri, M., Cormier, M., and Goddard, J.P. (2022). Squaraines as near-infrared photocatalysts for organic reactions. *Chem. Commun.* 58, 13759–13762. <https://doi.org/10.1039/d2cc04707a>.

68. Gao, Q., Tu, K., Li, H., Zhang, L., and Cheng, Z. (2021). A novel reversible-deactivation radical polymerization strategy via near-infrared light-controlled photothermal conversion dividing wall-type heat exchanger. *Sci. China Chem.* 64, 1242–1250. <https://doi.org/10.1007/s11426-021-1002-1>.

69. Nikoloudakis, E., López-Duarte, I., Charalambidis, G., Ladomenou, K., Ince, M., and Coutsolelos, A.G. (2022). Porphyrins and phthalocyanines as biomimetic tools for photocatalytic H₂ production and CO₂ reduction. *Chem. Soc. Rev.* 51, 6965–7045. <https://doi.org/10.1039/d2cs00183g>.

70. Zhang, Y., Ren, K., Wang, L., Wang, L., and Fan, Z. (2022). Porphyrin-based heterogeneous photocatalysts for solar energy conversion. *Chin. Chem. Lett.* 33, 33–60. <https://doi.org/10.1016/j.ccl.2021.06.013>.

71. Rybicka-Jasińska, K., Wdowik, T., Łuczak, K., Wierzba, A.J., Drapała, O., and Gryko, D. (2022). Porphyrins as promising photocatalysts for red-light-induced functionalizations of biomolecules. *ACS Org. Inorg. Au* 2, 422–426. <https://doi.org/10.1021/acsgorinorgau.2c00025>.

72. Lee, J., Papatzimas, J.W., Bromby, A.D., Gorobets, E., and Derkson, D.J. (2016). Thiaporphyrin-mediated photocatalysis using red light. *RSC Adv.* 6, 59269–59272. <https://doi.org/10.1039/c6ra11374e>.

73. Zhou, W., Uttronkrie, N.J., Lessard, B.H., and Brusso, J.L. (2021). From chemical curiosity to versatile building blocks: unmasking the hidden potential of main-group phthalocyanines in organic field-effect transistors. *Mater. Adv.* 2, 165–185. <https://doi.org/10.1039/d0ma00864h>.

74. Nyokong, T. (2007). Effects of substituents on the photochemical and photophysical properties of main group metal phthalocyanines. *Coord. Chem. Rev.* 251, 1707–1722. <https://doi.org/10.1016/j.ccr.2006.11.011>.

75. Lancel, M., Golisano, T., Monnereau, C., Gomez, C., Port, M., and Amara, Z. (2023). Sustainable Photooxidation using a Subpart-per-million Heavy-Metal-Free Red-Light Photocatalyst. *ACS Sustain. Chem. Eng.* 11, 15674–15684. <https://doi.org/10.1021/acssuschemeng.3c04688>.

76. Matsuzaki, K., Hiromura, T., Tokunaga, E., and Shibata, N. (2017). Trifluoroethoxy-coated subphthalocyanine affects trifluoromethylation of alkenes and alkynes even under low-energy red-light irradiation. *Chemistry (Rajkot, India)* 6, 226–230. <https://doi.org/10.1002/open.201600172>.

77. Yan, P., Zeng, R., Bao, B., Yang, X.-M., Zhu, L., Pan, B., Niu, S.-L., Qi, X.-W., Li, Y.-L., and Ouyang, Q. (2022). Red light induced highly efficient aerobic oxidation of organoboron compounds using spinach as a photocatalyst. *Green Chem.* 24, 9263–9268. <https://doi.org/10.1039/d2gc03055a>.

78. Buksh, B.F., Knutson, S.D., Oakley, J.V., Bissonnette, N.B., Oblinsky, D.G., Schwoerer, M.P., Seath, C.P., Geri, J.B., Rodriguez-Rivera, F.P., Parker, D.L., et al. (2022). μ Map-Red: proximity labeling by red light photocatalysis. *J. Am. Chem. Soc.* 144, 6154–6162. <https://doi.org/10.1021/jacs.2c01384>.

79. Wu, Z., Jung, K., and Boyer, C. (2020). Effective utilization of NIR wavelengths for photo-controlled polymerization: penetration through thick barriers and parallel solar syntheses. *Angew. Chem. Int. Ed.* 59, 2013–2017. <https://doi.org/10.1002/anie.201912484>.

80. Ishikawa, Y., Kameyama, T., Torimoto, T., Maeda, H., Segi, M., and Furuyama, T. (2021). Red-light-activatable ruthenium phthalocyanine catalysts. *Chem. Commun.* 57, 13594–13597. <https://doi.org/10.1039/d1cc06307c>.

81. Yerien, D.E., Cooke, M.V., García Vior, M.C., Barata-Vallejo, S., and Postigo, A. (2019). Radical fluoroalkylation reactions of (hetero) arenes and sulfides under red light photocatalysis. *Org. Biomol. Chem.* 17, 3741–3746. <https://doi.org/10.1039/c9ob00486f>.

82. Katsurayama, Y., Ikabata, Y., Maeda, H., Segi, M., Nakai, H., and Furuyama, T. (2022). Direct near infrared light-activatable phthalocyanine catalysts. *Chem. Eur. J.* 28, e202103223. <https://doi.org/10.1002/chem.202103223>.

83. Grundke, C., Silva, R.C., Kitzmann, W.R., Heinze, K., de Oliveira, K.T., and Opatz, T. (2022). Photochemical α -aminonitrile synthesis using Zn-phthalocyanines as near-infrared photocatalysts. *J. Org. Chem.* 87, 5630–5642. <https://doi.org/10.1021/acs.joc.1c03101>.

84. Sun, J., Ren, S., Zhao, H., Zhang, S., Xu, X., Zhang, L., and Cheng, Z. (2023). NIR-photocontrolled aqueous RAFT polymerization with polymerizable water-soluble zinc phthalocyanine as photocatalyst. *ACS Macro Lett.* 12, 165–171. <https://doi.org/10.1021/acsmacrolett.2c00708>.

85. Ravetz, B.D., Tay, N.E.S., Joe, C.L., Sezen-Edmonds, M., Schmidt, M.A., Tan, Y., Janey, J.M., Eastgate, M.D., and Rovis, T. (2020). Development of a platform for near-infrared photoredox catalysis. *ACS Cent. Sci.* 6, 2053–2059. <https://doi.org/10.1021/acscentsci.0c00948>.

86. Goldschmid, S.L., Bednárová, E., Beck, L.R., Xie, K., Tay, N.E.S., Ravetz, B.D., Li, J., Joe, C.L., and Rovis, T. (2022). Tuning the electrochemical and photophysical properties of osmium-based photoredox catalysts. *Synlett* 33, 247–258. <https://doi.org/10.1055/s-0041-1737792>.

87. Goldschmid, S.L., Soon Tay, N.E., Joe, C.L., Lainhart, B.C., Sherwood, T.C., Simmons, E.M., Sezen-Edmonds, M., and Rovis, T. (2022). Overcoming photochemical limitations in metallaphotoredox catalysis: red-light-driven C–N cross-coupling. *J. Am. Chem. Soc.* 144, 22409–22415. <https://doi.org/10.1021/jacs.2c09745>.

88. Tay, N.E.S., Ryu, K.A., Weber, J.L., Olow, A.K., Cabanero, D.C., Reichman, D.R., Oslund, R.C., Fadeyi, O.O., and Rovis, T. (2023). Targeted activation in localized protein environments via deep red photoredox catalysis. *Nat. Chem.* 15, 101–109. <https://doi.org/10.1038/s41557-022-01057-1>.

89. Cabanero, D.C., Kariofillis, S.K., Johns, A.C., Kim, J., Ni, J., Park, S., Parker, D.L., Jr., Ramil, C.P., Roy, X., Shah, N.H., and Rovis, T. (2024). Photocatalytic Activation of Aryl

(trifluoromethyl) Diazos to Carbenes for High-Resolution Protein Labeling with Red Light. *J. Am. Chem. Soc.* 146, 1337–1345. <https://doi.org/10.1021/jacs.3c09545>.

90. Ogbu, I.M., Bassani, D.M., Robert, F., and Landais, Y. (2022). Photocatalyzed decarboxylation of oxamic acids under near-infrared conditions. *Chem. Commun.* 58, 8802–8805. <https://doi.org/10.1039/d2cc03155h>.

91. Teply, F. (2011). Photoredox catalysis by $[\text{Ru}(\text{bpy})_3]^{2+}$ to trigger transformations of organic molecules. *Organic synthesis using visible-light photocatalysis and its 20th century roots. Collect. Czech Chem. Commun.* 76, 859–917. <https://doi.org/10.1135/cccc2011078>.

92. Rupp, M.T., Auvray, T., Shevchenko, N., Swoboda, L., Hanan, G.S., and Kurth, D.G. (2021). Substituted 2,4-di(pyridin-2-yl) pyrimidine-based ruthenium photosensitizers for hydrogen photoevolution under red light. *Inorg. Chem.* 60, 292–302. <https://doi.org/10.1021/acs.inorgchem.0c02955>.

93. Whittemore, T.J., Xue, C., Huang, J., Gallucci, J.C., and Turro, C. (2020). Single-chromophore single-molecule photocatalyst for the production of dihydrogen using low-energy light. *Nat. Chem.* 12, 180–185. <https://doi.org/10.1038/s41557-019-0397-4>.

94. Millet, A., Xue, C., Turro, C., and Dunbar, K.R. (2021). Unsymmetrical dirhodium single molecule photocatalysts for H_2 production with low energy light. *Chem. Commun.* 57, 2061–2064. <https://doi.org/10.1039/d0cc08248a>.

95. Huang, J., Sun, J., Wu, Y., and Turro, C. (2021). Dirhodium(II,II)/NiO photocathode for photoelectrocatalytic hydrogen evolution with red light. *J. Am. Chem. Soc.* 143, 1610–1617. <https://doi.org/10.1021/jacs.0c12171>.

96. Su, X.D., Liu, Q., Li, X.N., Zhang, B.B., Wang, Z.X., and Chen, X.Y. (2023). Near-infrared-light-induced iron (I) dimer-enabled halogen atom transfer for rapid iodoperfluoroalkylation of alkenes. *Chem. Catal.* 3, 100710. <https://doi.org/10.1016/j.chechat.2023.100710>.

97. Huang, L., Wu, W., Li, Y., Huang, K., Zeng, L., Lin, W., and Han, G. (2020). Highly effective near-infrared activating triplet-triplet annihilation upconversion for photoredox catalysis. *J. Am. Chem. Soc.* 142, 18460–18470. <https://doi.org/10.1021/jacs.0c06976>.

98. Ye, C., Zhou, L., Wang, X., and Liang, Z. (2016). Photon upconversion: from two-photon absorption (TPA) to triplet-triplet annihilation (TTA). *Phys. Chem. Chem. Phys.* 18, 10818–10835. <https://doi.org/10.1039/c5cp07296d>.

99. Glaser, F., Kerzig, C., and Wenger, O.S. (2020). Multi-photon excitation in photoredox catalysis: concepts, applications, methods. *Angew. Chem. Int. Ed.* 59, 10266–10284. <https://doi.org/10.1002/anie.201915762>.

100. Zeng, L., Huang, L., Han, J., and Han, G. (2022). Enhancing triplet-triplet annihilation upconversion: from molecular design to present applications. *Acc. Chem. Res.* 55, 2604–2615. <https://doi.org/10.1021/acs.accounts.2c00307>.

101. Ravetz, B.D., Pun, A.B., Churchill, E.M., Congreve, D.N., Rovis, T., and Campos, L.M. (2019). Photoredox catalysis using infrared light via triplet fusion upconversion. *Nature* 565, 343–346. <https://doi.org/10.1038/s41586-018-0835-2>.

102. Zeng, L., Huang, L., Lin, W., Jiang, L.H., and Han, G. (2023). Red light-driven electron sacrificial agents-free photoreduction of inert aryl halides via triplet-triplet annihilation. *Nat. Commun.* 14, 1102. <https://doi.org/10.1038/s41467-023-36679-7>.

103. Liu, S., Liu, H., Shen, L., Xiao, Z., Hu, Y., Zhou, J., Wang, X., Liu, Z., Li, Z., and Li, X. (2022). Applying triplet-triplet annihilation upconversion in degradation of oxidized lignin model with good selectivity. *Chem. Eng. J.* 431, 133377. <https://doi.org/10.1016/j.cej.2021.133377>.

104. Huang, L., Zeng, L., Chen, Y., Yu, N., Wang, L., Huang, K., Zhao, Y., and Han, G. (2021). Long wavelength single photon like driven photolysis via triplet triplet annihilation. *Nat. Commun.* 12, 122. <https://doi.org/10.1038/s41467-020-20326-6>.

105. Lv, W., Li, Y., Li, F., Lan, X., Zhang, Y., Du, L., Zhao, Q., Phillips, D.L., and Wang, W. (2019). Upconversion-like photolysis of BODIPY-based prodrugs via a one-photon process. *J. Am. Chem. Soc.* 141, 17482–17486. <https://doi.org/10.1021/jacs.9b09034>.

106. Long, K., Han, H., Kang, W., Lv, W., Wang, L., Wang, Y., Ge, L., and Wang, W. (2021). One-photon red light-triggered disassembly of small-molecule nanoparticles for drug delivery. *J. Nanobiotechnology* 19, 357. <https://doi.org/10.1186/s12951-021-01103-z>.

107. Long, K., Lv, W., Wang, Z., Zhang, Y., Chen, K., Fan, N., Li, F., Zhang, Y., and Wang, W. (2023). Near-infrared light-triggered prodrug photolysis by one-step energy transfer. *Nat. Commun.* 14, 8112. <https://doi.org/10.1038/s41467-023-43805-y>.

108. Herr, P., Glaser, F., Büldt, L.A., Larsen, C.B., and Wenger, O.S. (2019). Long-lived, strongly emissive, and highly reducing excited states in Mo (0) complexes with chelating isocyanides. *J. Am. Chem. Soc.* 141, 14394–14402. <https://doi.org/10.1021/jacs.9b07373>.

109. Bilger, J.B., Kerzig, C., Larsen, C.B., and Wenger, O.S. (2021). A photorobust Mo(0) complex mimicking $[\text{Os}(2',2'\text{-bipyridine})_3]^{2+}$ and its application in red-to-blue upconversion. *J. Am. Chem. Soc.* 143, 1651–1663. <https://doi.org/10.1021/jacs.0c12805>.

110. Glaser, F., and Wenger, O.S. (2022). Sensitizer-controlled photochemical reactivity via upconversion of red light. *Chem. Sci.* 14, 149–161. <https://doi.org/10.1039/d2sc05229f>.

111. Liang, W., Nie, C., Du, J., Han, Y., Zhao, G., Yang, F., Liang, G., and Wu, K. (2023). Near-infrared photon upconversion and solar synthesis using lead-free nanocrystals. *Nat. Photonics* 17, 346–353. <https://doi.org/10.1038/s41566-023-01156-6>.

112. Choi, D., Nam, S.K., Kim, K., and Moon, J.H. (2019). Enhanced photoelectrochemical water splitting through bismuth vanadate with a photon upconversion luminescent reflector. *Angew. Chem. Int. Ed.* 58, 6891–6895. <https://doi.org/10.1002/anie.201813440>.

113. Yu, T., Liu, Y., Zeng, Y., Chen, J., Yang, G., and Li, Y. (2019). Triplet-triplet annihilation upconversion for photocatalytic hydrogen evolution. *Chem. Eur. J.* 25, 16270–16276. <https://doi.org/10.1002/chem.201904025>.

114. Luo, G., Liu, Y., Zeng, Y., Yu, T., Chen, J., Hu, R., Yang, G., and Li, Y. (2022). Enhancing photon upconversion with thermally activated sensitization and singlet energy collection. *J. Mater. Chem. C* 10, 8596–8601. <https://doi.org/10.1039/d2tc00766e>.

115. Glaser, F., and Wenger, O.S. (2022). Red light-based dual photoredox strategy resembling the Z-scheme of natural photosynthesis. *JACS Au* 2, 1488–1503. <https://doi.org/10.1021/jacsau.2c00265>.

116. Göppert, M. (1929). Über die Wahrscheinlichkeit des Zusammenwirkens zweier Lichtquanten in einem Elementarakt. *Sci. Nat.* 17, 932. <https://doi.org/10.1007/BF01506585>.

117. Göppert-Mayer, M. (1931). Über Elementarakte mit zwei Quantensprüngen. *Ann. Phys.* 401, 273–294. <https://doi.org/10.1002/andp.19314010303>.

118. Kaiser, W., and Garrett, C.G.B. (1961). Two-photon excitation in $\text{CaF}_2:\text{Eu}^{2+}$. *Phys. Rev. Lett.* 7, 229. <https://doi.org/10.1103/PhysRevLett.7.229>.

119. Patterson, G.H., and Piston, D.W. (2000). Photobleaching in two-photon excitation microscopy. *Biophys. J.* 78, 2159–2162.

120. Pawlicki, M., Collins, H.A., Denning, R.G., and Anderson, H.L. (2009). Two-photon absorption and the design of two-photon dyes. *Angew. Chem. Int. Ed.* 48, 3244–3266. <https://doi.org/10.1002/anie.200805257>.

121. Shaw, P.A., Forsyth, E., Haseeb, F., Yang, S., Bradley, M., and Klausen, M. (2022). Two-photon Absorption: an open door to the NIR-II biological window? *Front. Chem.* 10, 921354. <https://doi.org/10.3389/fchem.2022.921354>.

122. Zhang, K., Sun, Y., Wu, S., Zhou, M., Zhang, X., Zhou, R., Zhang, T., Gao, Y., Chen, T., Chen, Y., et al. (2021). Systematic imaging in medicine: a comprehensive review. *Eur. J. Nucl. Med. Mol. Imag.* 48, 1736–1758. <https://doi.org/10.1007/s00259-020-05107-z>.

123. Chen, R., Wang, L., Ding, G., Han, G., Qiu, K., Sun, Y., and Diao, J. (2023). Constant conversion rate of endolysosomes revealed by a pH-sensitive fluorescent probe. *ACS Sens.* 8, 2068–2078. <https://doi.org/10.1021/acssensors.3c00340>.

124. Mizuta, Y. (2021). Advances in two-photon imaging in plants. *Plant Cell Physiol.* 62, 1224–1230. <https://doi.org/10.1093/pcp/pcab062>.

125. Chen, R., Qiu, K., Leong, D.C.Y., Kundu, B.K., Zhang, C., Srivastava, P., White, K.E., Li, G., Han, G., Guo, Z., et al. (2023). A general design of pyridinium-based fluorescent probes for enhancing two-photon microscopy. *Biosens. Bioelectron.* 239, 115604. <https://doi.org/10.1016/j.bios.2023.115604>.

126. Makarov, N.S., Rebane, A., Drobizhev, M., Wolleb, H., and Spahni, H. (2007). Optimizing two-photon absorption for volumetric optical data storage. *J. Opt. Soc. Am. B* 24, 1874–1885. <https://doi.org/10.1364/JOSAB.24.001874>.

127. McKenzie, L.K., Sazanovich, I.V., Baggaley, E., Bonneau, M., Guerchais, V., Williams, J.A.G., Weinstein, J.A., and Bryant, H.E. (2017). Metal complexes for two-photon photodynamic therapy: a cyclometallated iridium complex induces two-photon photosensitization of cancer cells under near-IR light. *Chem. Eur. J.* 23, 234–238. <https://doi.org/10.1002/chem.201604792>.

128. Shen, Y., Shuhendler, A.J., Ye, D., Xu, J.-J., and Chen, H.-Y. (2016). Two-photon excitation nanoparticles for photodynamic therapy. *Chem. Soc. Rev.* 45, 6725–6741. <https://doi.org/10.1039/C6CS00442C>.

129. Ogawa, K., and Kobuke, Y. (2008). Recent advances in two-photon photodynamic therapy. *Anti Cancer Agents Med. Chem.* 8, 269–279. <https://doi.org/10.2174/187152008783961860>.

130. Li, H., Yang, Y., He, C., Zeng, L., and Duan, C. (2018). Mixed-ligand metal-organic framework for two-photon responsive photocatalytic C–N and C–C coupling reactions. *ACS Catal.* 9, 422–430. <https://doi.org/10.1021/acscatal.8b03537>.

131. Han, G., Li, G., Huang, J., Han, C., Turro, C., and Sun, Y. (2022). Two-photon-absorbing ruthenium complexes enable near infrared light-driven photocatalysis. *Nat. Commun.* 13, 2288. <https://doi.org/10.1038/s41467-022-29981-3>.

132. Tang, J.H., Han, G., Li, G., Yan, K., and Sun, Y. (2022). Near-infrared light photocatalysis enabled by a ruthenium complex-integrated metal-organic framework via two-photon absorption. *iScience* 25, 104064. <https://doi.org/10.1016/j.isci.2022.104064>.

133. Kundu, B.K., Han, C., Srivastava, P., Nagar, S., White, K.E., Krause, J.A., Elles, C.G., and Sun, Y. (2023). Trifluoromethylative bifunctionalization of alkenes via a bibenzothiazole-derived photocatalyst under both visible- and near-infrared-light irradiation. *ACS Catal.* 13, 8119–8127. <https://doi.org/10.1021/acscatal.3c01812>.

134. Kundu, B.K., Han, G., and Sun, Y. (2023). Derivatized benzothiazoles as two-photon-absorbing organic photosensitizers active under near infrared light irradiation. *J. Am. Chem. Soc.* 145, 3535–3542. <https://doi.org/10.1021/jacs.2c12244>.

135. Yu, J., Cui, Y., Wu, C.D., Yang, Y., Chen, B., and Qian, G. (2015). Two-photon responsive metal-organic framework. *J. Am. Chem. Soc.* 137, 4026–4029. <https://doi.org/10.1021/ja512552g>.

136. Karges, J., Kuang, S., Maschietto, F., Blacque, O., Ciofini, I., Chao, H., and Gasser, G. (2020). Rationally designed ruthenium complexes for 1- and 2-photon photodynamic therapy. *Nat. Commun.* 11, 3262. <https://doi.org/10.1038/s41467-020-16993-0>.

137. Takematsu, K., Wehlin, S.A.M., Sattler, W., Winkler, J.R., and Gray, H.B. (2017). Two-photon spectroscopy of tungsten(0) arylisocyanides using nanosecond-pulsed excitation. *Dalton Trans.* 46, 13188–13193. <https://doi.org/10.1039/c7dt02632c>.

138. Fajardo, J., Jr., Barth, A.T., Morales, M., Takase, M.K., Winkler, J.R., and Gray, H.B. (2021). Photoredox catalysis mediated by tungsten(0) arylisocyanides. *J. Am. Chem. Soc.* 143, 19389–19398. <https://doi.org/10.1021/jacs.1c07617>.

139. Romero Ávila, M., León-Rojas, A.F., Lacroix, P.G., Malfant, I., Farfán, N., Mhanna, R., Santillan, R., Ramos-Ortiz, G., and Malval, J.P. (2020). Two-photon-triggered NO release via a ruthenium-nitrosyl complex with a star-shaped architecture. *J. Phys. Chem. Lett.* 11, 6487–6491. <https://doi.org/10.1021/acs.jpclett.0c01953>.

140. Lin, M., Zou, S., Liao, X., Chen, Y., Luo, D., Ji, L., and Chao, H. (2021). Ruthenium(II) complexes as bioorthogonal two-photon photosensitizers for tumour-specific photodynamic therapy against triple-negative breast cancer cells. *Chem. Commun.* 57, 4408–4411. <https://doi.org/10.1039/d1cc00661d>.

141. Santiko, E.B., Babu, S.B., Zhang, F., Wu, C.-L., Lin, T.-C., and Abe, M. (2023). Synthesis, characterization, and application of a cyclic stilbene derivative with simultaneous two-photon absorption character. *Chem. Lett.* 52, 846–849. <https://doi.org/10.1246/cl.230388>.